

Bloch Oscillations in Optical and Zeeman Lattices in the Presence of Spin-Orbit Coupling

Yaroslav V. Kartashov^{1,2}, Vladimir V. Konotop³, Dmitry A. Zezyulin³, and Lluís Torner^{1,4}

¹ *ICFO-Institut de Ciències Fotoniques, The Barcelona Institute of Science and Technology, 08860 Castelldefels (Barcelona), Spain*

² *Institute of Spectroscopy, Russian Academy of Sciences, Troitsk, Moscow Region, 142190, Russia*

³ *Centro de Física Teórica e Computacional, Faculdade de Ciências and Departamento de Física, Faculdade de Ciências, Universidade de Lisboa, Campo Grande, Ed. C8, Lisboa 1749-016, Portugal and*

⁴ *Universitat Politècnica de Catalunya, 08034 Barcelona, Spain*

(Dated: October 20, 2016)

We address Bloch oscillations of a spin-orbit coupled atom in periodic potentials of two types: Optical and Zeeman lattices. We show that in optical lattices the spin-orbit coupling allows controlling the direction of atomic motion and may lead to complete suppression of the oscillations at specific values of the coupling strength. In Zeeman lattices the energy bands are found to cross each other at the boundaries of the Brillouin zone, resulting in period-doubling of the oscillations. In all cases, the oscillations are accompanied by rotation of the pseudo-spin, with a dynamics that is determined by the strength of the spin-orbit coupling. The predicted effects are discussed also in terms of a Wannier-Stark ladder, which in optical lattices consist of two mutually-shifted equidistant sub-ladders.

PACS numbers: 37.10.Jk, 32.60.+i, 03.75.-b

Bloch oscillations (BOs) of electrons in a crystal under the action of a constant electric field [1] is one of the fundamental predictions of quantum mechanics. They were observed in semiconductor superlattices [2, 3], a few years after the observation [4] of a Wannier-Stark ladder (WSL). BOs have been observed in a variety of systems where waves can propagate in periodic environment [5], such as cold atoms [6], Bose-Einstein condensates (BECs) [7] held in optical lattices, and diverse optical settings, including waveguide arrays [8], optically-induced lattices [9], coupled microcavities [10], or plasmonic systems [11].

To date, most studies about BOs in atomic systems have addressed one-component settings. Two-component systems have received less attention. A particularly interesting situation occurs in the presence of linear coupling between components that in steady state locks their energies. Spin-orbit (SO) coupling can be implemented in a multi-level atom [12] for which artificial electric [13] and magnetic [14, 15] fields can be created by managing interactions between different hyperfine states [16]. A system involving coupled hyperfine atomic states in a periodic potential and subjected to linear forces induced by a Zeeman field undergo BOs [17] in a static field or quantum walks in a time-periodic field. The dynamics of such a system is strongly influenced by the presence of two oppositely tilted WSL in the eigenmode spectrum [18]. Interesting dynamical regimes occur in SO-coupled BECs [19]. The interplay of BOs due to a linear force and the spin Hall effect induced by the SO coupling can lead to complex evolution of BECs in a two-dimensional lattice [20]. Both, BOs and WSL of a four-component model of a helicoidal molecule with SO coupling have been addressed [21].

In this Letter we report unconventional features that SO coupling brings into the dynamics of BOs in a system held either in an optical lattice (OL) or in a Zeeman lattice (ZL) and subjected to a linear force. We highlight suppression of BOs due to band-flattening in optical lattices, transition from periodic to non-periodic BOs, period-doubling of BOs in Zeeman lattices due to band-crossing at the edges of the Brillouin zone (BZ), and control of the direction of motion of broad wavepackets.

We consider a two-level atom described by the spinor $\Psi = (\Psi_1, \Psi_2)^T$, which solves the Schrödinger equation $i\Psi_t = (H_0 + H_L + \beta x)\Psi$, where time and position are measured respectively in units of $2md^2/(\hbar\pi^2)$ and d/π , with m being the mass of the atom and d the lattice period. $H_0 = p^2 + \gamma\sigma_3 p + \Omega_1\sigma_1$ is the Hamiltonian without lattice and external field, $p = -i\partial/\partial x$ is the momentum, γ is the SO coupling strength, Ω_1 is the Rabi frequency, β is the linear force, and $\sigma_{1,2,3}$ are Pauli matrices. The potential $H_L(x)$ is set by an OL $H_L(x) = V(x)$ that is equal for both spinor components, or by a ZL $H_L(x) = \Omega_3(x)\sigma_3$ having opposite signs for the components. Both lattices are π -periodic, i.e., $H_L(x) = H_L(x + \pi)$; even functions with respect to the origin [$H_L(x) = H_L(-x)$]; and odd functions with respect to the quarter-period [$H_L(\pi/4 + x) = -H_L(\pi/4 - x)$]. In simulations we model OLs and ZLs as $V(x) = -4\cos(2x)$ and $\Omega_3(x) = 4\cos(2x)$, respectively [see Fig. 1]. Both such potentials are experimentally feasible as described in Refs. [7] and [22] for OLs and ZLs, respectively.

When $\beta = 0$, the eigenmodes of the system are Bloch waves $\Psi = \psi_k e^{-i\mu(k)t}$, i.e., $(H_0 + H_L)\psi_k = \mu(k)\psi_k$, where $\psi_k = \mathbf{u}_k(x)e^{ikx}$, $\mathbf{u}_k(x) = \mathbf{u}_k(x + \pi)$, and k is the Bloch momentum in the reduced BZ: $k \in [-1, +1]$. We start with a semi-classical description valid for broad

wavepackets (namely, $\delta k d \ll 1$, where δk is the spectral width of the wavepacket). Similarly to the one-component case [1, 23], one can show [24] that if the linear force is weak, $\beta \ll 1$, and the inter-band tunneling is negligible, the center of a wavepacket $x_c(t) = \int_{-\infty}^{\infty} \Psi^\dagger x \Psi dx$, initially chosen as a Bloch wave modulated by an envelope ensuring $\int_{-\infty}^{\infty} \Psi^\dagger \Psi dx = 1$, behaves as $dx_c/dt = (\partial \mu(k)/\partial k)_{k=k_0-\beta t}$. Hence

$$x_c(t) = x_0 + \frac{1}{\beta} [\mu(k_0) - \mu(k_0 - \beta t)] \quad (1)$$

where x_0 and k_0 are the initial coordinate and Bloch momentum, respectively. Since the BZ width is 2, the wavepacket crosses the zone after the time interval $2/\beta$.

Important information about the Bloch modes can be obtained from the symmetries of the Hamiltonian [25]. Starting with OLs, we recall [26] that the Hamiltonian $H_{\text{OL}} = H_0 + V(x)$ obeys the Klein four-group symmetry $\{\hat{1}, \alpha_1, \alpha_2, \alpha_3\}$, i.e., $[H_{\text{OL}}, \alpha_j] = 0$, defined by the operators $\alpha_1 = \sigma_1 \mathcal{P}$, $\alpha_2 = \sigma_1 \mathcal{T}$, and $\alpha_3 = \mathcal{P}\mathcal{T}$, where \mathcal{T} is the time reversal operator, $\mathcal{T}\psi(x) = \psi^*(x)$, \mathcal{P} is the parity operator with respect to $x = 0$, i.e., $\mathcal{P}\psi(x) = \psi(-x)$ and $\hat{1}$ is the identity operator. Here $\alpha_i \alpha_j = \alpha_k$, where i, j and k are all different. In terms of the Bloch modes ψ_k , the operators \mathcal{P} and \mathcal{T} map a state at k to a state at $-k$: $\mathcal{P}\mathbf{u}_k = \mathbf{u}_k(-x) = \mathbf{u}_{-k}(x)$ and $\mathcal{T}\mathbf{u}_k = \mathbf{u}_k^*(x) = \mathbf{u}_{-k}(x)$. Thus α_1 and α_2 symmetries imply $k \rightarrow -k$ mapping, while α_3 does not affect k . At least one of the eigenfunctions of H_{OL} obeys *all* α -symmetries. When at the boundary ($k = 1$) [at the center ($k = 0$)] of the BZ energy levels do not cross each other, the eigenvalue $\mu(1)$ [$\mu(0)$] is non-degenerate and its eigenfunction is highly symmetric. Such eigenfunction must satisfy $\alpha_2 \psi_k = \psi_k$ with $k = 1$ [$k = 0$], and hence $|u_{1,k}| = |u_{2,k}|$. In terms of the average values of the pseudo-spin (or spin, for brevity) components $S_j = \int_{-\pi}^{\pi} \psi^\dagger \sigma_j \psi dx$ ($S_j = \int_{-\infty}^{\infty} \Psi^\dagger \sigma_j \Psi dx$ for localized nonstationary solutions), this means that at the boundary [center] of the BZ $S_3 = 0$. Such phenomenon is observed in the dynamical simulations shown in Fig. 3.

In ZLs only one ($\alpha_3 = \mathcal{P}\mathcal{T}$) of the above symmetries remains, but there appears an additional one: $\tilde{\alpha}_1 = \sigma_1 \tilde{\mathcal{P}}$, where $\tilde{\mathcal{P}}$ is the reflection with respect to $x = \pi/4$. Consider an eigenstate at the BZ boundary, $\psi^{\text{BZ}} = \psi_{k=1}$, and assume that its eigenvalue is nondegenerate (which implies that no crossing of the energy levels occurs at $k = 1$). It can be chosen to be either α_3 -symmetric $\psi^{\text{BZ}} = \alpha_3 \psi^{\text{BZ}}$, or satisfying $\tilde{\psi}^{\text{BZ}} = \pm \tilde{\alpha}_1 \tilde{\psi}^{\text{BZ}}$. We set the “+” sign (the sign “−” is analogous). Non-degeneracy implies the linear dependence $\psi^{\text{BZ}} = c \tilde{\psi}^{\text{BZ}}$ where c is a complex number, and means that $\psi^{\text{BZ}} = \tilde{\alpha}_1 \psi^{\text{BZ}}$ because $\tilde{\alpha}_1$ is linear. Thus ψ^{BZ} is simultaneously α_3 and $\tilde{\alpha}_1$ -symmetric: $\psi^{\text{BZ}} = \tilde{\alpha}_1 \psi^{\text{BZ}} = \alpha_3 \psi^{\text{BZ}}$. Using Floquet’s theorem we obtain: $\psi_j^{\text{BZ}}(\frac{\pi}{4} - x) = [\psi_j^{\text{BZ}}(x - \frac{\pi}{4})]^* = \psi_{3-j}^{\text{BZ}}(\frac{\pi}{4} + x) = -\psi_j^{\text{BZ}}(-\frac{3\pi}{4} - x)$. The ansatz $x \rightarrow x - \frac{\pi}{2}$ from the last equality yields $\psi_{3-j}^{\text{BZ}}(x - \frac{\pi}{4}) = -\psi_j^{\text{BZ}}(-\frac{\pi}{4} - x)$ for

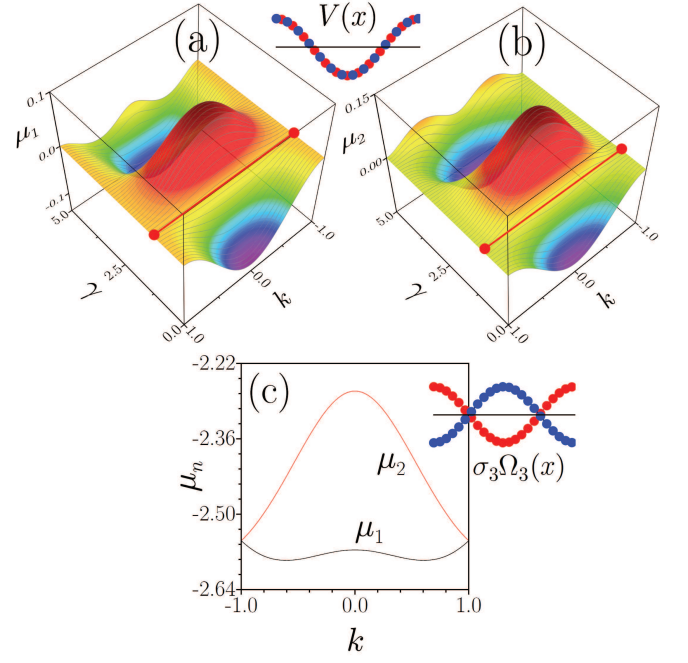


FIG. 1: (Color online) First (a) and second (b) bands in the OL spectrum as functions of γ . A vertical shift of the bands with increasing γ was eliminated by subtracting $\mu_n(k = 1)$ from $\mu_n(k)$. The red lines indicate some of the points where band flattening occurs. (c) First two bands in the spectrum of ZL at $\gamma = 2$. The top and bottom insets show OL and ZL and the blue and red dots correspond to the potentials affecting different components.

($j = 1, 2$), which means that $\psi^{\text{BZ}} = -\tilde{\alpha}_1 \psi^{\text{BZ}}$. This contradicts the assumption that the energy levels do not cross each other at $k = 1$ and that the $\tilde{\alpha}_1$ -symmetric state $\psi_{k=1}$ is nondegenerate. Therefore, the energy levels should cross at the boundary of the BZ. Note that $\tilde{\mathcal{P}}$ reflects the states with respect to the BZ origin (i.e., maps $k \rightarrow -k$) with simultaneous inversion of the spinor components. This means that S_3 has opposite signs at the k and $-k$ points.

The spectra for OL and ZL are illustrated in Fig. 1. Panels (a) and (b) show transformation of the first (μ_1) and second (μ_2) bands of the OL spectrum upon increase of the SO coupling. Panel (c) shows the two lowest bands $\mu_{1,2}$ of the ZL at $\gamma = 2$. For both types of lattices, increasing SO coupling leads to the appearance of extrema of $\mu(k)$ in the internal points of the BZ. In OLs, the slope of the $\mu_n(k)$ dependence may change its sign with increasing γ . According to (1) this means that the SO coupling may *invert* the direction of motion of the wavepacket. At a certain $\gamma = \gamma_f$ [red lines in Fig. 1 (a,b)] either the first or the second bands may become nearly flat. Namely, $\gamma_f = 1.17, 3.08$ for the first band, and $\gamma_f = 0.82, 2.93$ for the second band, and note that these values only slightly decrease with growth of the lattice depth. Such an extreme band-flattening, discussed

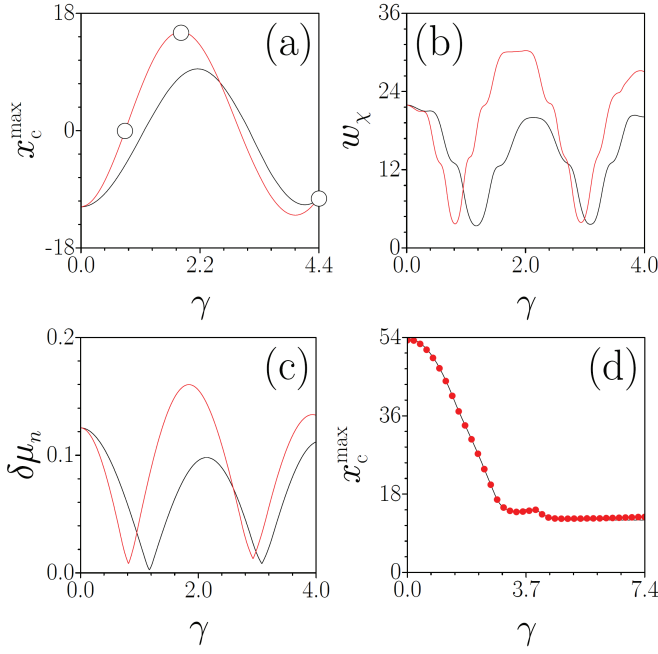


FIG. 2: (Color online) (a) Maximal displacement of a broad wavepacket, with a width $w_{in} = 9\pi/2$, at $k_0 = 0$; (b) Maximal width of a narrow ($w_{in} = \pi/2$) wavepacket *vs* γ in an OL; (c) Width of the OL bands *vs* γ . The black and red curves correspond to the first and second bands, respectively. The circles in (a) correspond to the dynamics in Figs. 3(a)–(c). (d) Amplitude of BOs in ZLs *vs* γ for a broad wavepacket. The analytical prediction (red dots) is superimposed to the numerical results (black lines). In all panels $\beta = 2\Omega_1/31\pi$.

also in [27], implies a weakly dispersive propagation and *almost complete suppression of BOs*. Indeed, according to (1) the amplitude of BOs for an atom in the n th band is given by $x_c^{\max} = [\max_k \mu_n(k) - \min_k \mu_n(k)]/\beta$ and it must be a nonmonotonic function of γ , consistent with Figs. 1(a,b). Band crossing at the edges of the BZ in ZLs is visible in Fig. 1(c).

The trajectory (1) is in excellent agreement with the direct solution of the Schrödinger equation using a Crank-Nicolson method. Calculations were conducted with 2×10^4 transverse points and steps $dx = 0.02$, $dt = 0.001$. The input broad wavepacket had the form $\Psi = \psi_k(x) \exp(-x^2/w_{in}^2)$, where $\psi_k(x)$ is the Bloch wave at $k = 0$ for a given γ . Fig. 2(a) illustrates the non-monotonic dependence of the maximal displacement x_c^{\max} , defined over 20 periods of BOs in an OL. x_c^{\max} becomes zero for specific values of the SO coupling γ , where we observe nearly complete suppression of BOs [Fig. 3(a)]. In contrast to broad wavepackets, strongly localized initial states do not experience displacement, but exhibit nearly periodic width oscillations in t , whose maximal amplitude $w_\chi = \max_t \{1/\int_{-\infty}^{\infty} (|\Psi_1|^4 + |\Psi_2|^4) dx\}$ is shown in Fig. 2(b) as a function of γ . Zeros of $x_c^{\max}(\gamma)$ and minima of $w_\chi(\gamma)$

coincide with the bandwidth minima from Fig. 2(c).

Figures 3(b,c) show that the SO coupling may change the direction of the wavepacket motion. For $\gamma > \gamma_f$ and $\gamma < \gamma_f$, a wavepacket initially corresponding to the Bloch mode with $k = 0$ moves in the opposite direction for a given linear force β . While the amplitudes of the BOs in Figs. 3(a,b) differ significantly, the spinor dynamics is similar and is characterized by the integral spin almost parallel to the SO coupling and exhibiting weak oscillations in the (x, z) -plane: $|S_1| \gg |S_{2,3}|$. Increasing the SO coupling results in rotation of the spin direction, which becomes nearly orthogonal to the SO coupling. In Fig. 3(c) the spin is mainly directed along the z -axis and $|S_3| \gg |S_{1,2}|$. Since flattening of different bands occurs for different values of γ [Fig. 2(c)], an arbitrary superposition of several band states always exhibits BOs.

The BOs dynamics changes drastically if the initial wavepacket is a superposition of states from more than one band. This phenomenon is illustrated in Fig. 3(d), which was obtained for the same parameters as Fig. 3(b) but now for a superposition of eigenmodes from the two lowest bands. Since a two-level atom is characterized by the Rabi frequency $\Omega_1 \gg \beta$, BOs with frequency $\pi\beta$ are accompanied by rapid oscillations between the spinor components, visible as spin rotation in the plane (y, z) , $|S_1| \ll 1$, whose frequency exceeds Ω_1 because of the effect of the SO coupling. Such evolution, characterized by two frequencies, can be strictly periodic only if the frequencies are commensurable, a case that corresponds to a fully equidistant WSL as discussed below.

The BOs dynamics in ZLs is substantially different than in OLs, due to two main features of the spectrum: (i) band crossing at BZ edges and (ii) vanishing of the S_3 spin-projection at $k = 0$ and inversion of S_3 at $k = \pm 1$. Such features have a direct impact on the BOs: the period of BOs in ZLs *doubles* in comparison to that encountered in OLs, and amounts to $4/\beta$. Indeed, a broad wavepacket starting its motion around $k = -1$ and moving along the lowest band still crosses the BZ after a time period $2/\beta$, but it arrives to the opposite edge of the BZ at $k = +1$ with an inverted S_3 component. Subsequently, it keeps moving along the *second* band, intersecting with the lowest band at $k = 1$ and only after passing the BZ again, but now along a new path, it returns to the original state after the total time interval of $4/\beta$ (see Fig. 4). As in the case of OLs, for a moderate SO coupling, the spin dynamics in ZLs is bound to the (x, z) plane ($|S_{1,3}| \gg |S_2|$). When γ grows the spin becomes orthogonal to the SO coupling [$|S_3| \gg |S_{1,2}|$ in Fig. 4(b)]. Thus the amplitude of the BOs in ZLs is determined by the combined width of the *two* lowest bands. This is confirmed by Fig. 2(d), which compares the BOs amplitude obtained numerically with the predictions of (1), but taking the combined width of the two lowest bands as a total range of variation of μ . The BOs amplitude in ZLs becomes independent of γ for a sufficiently strong

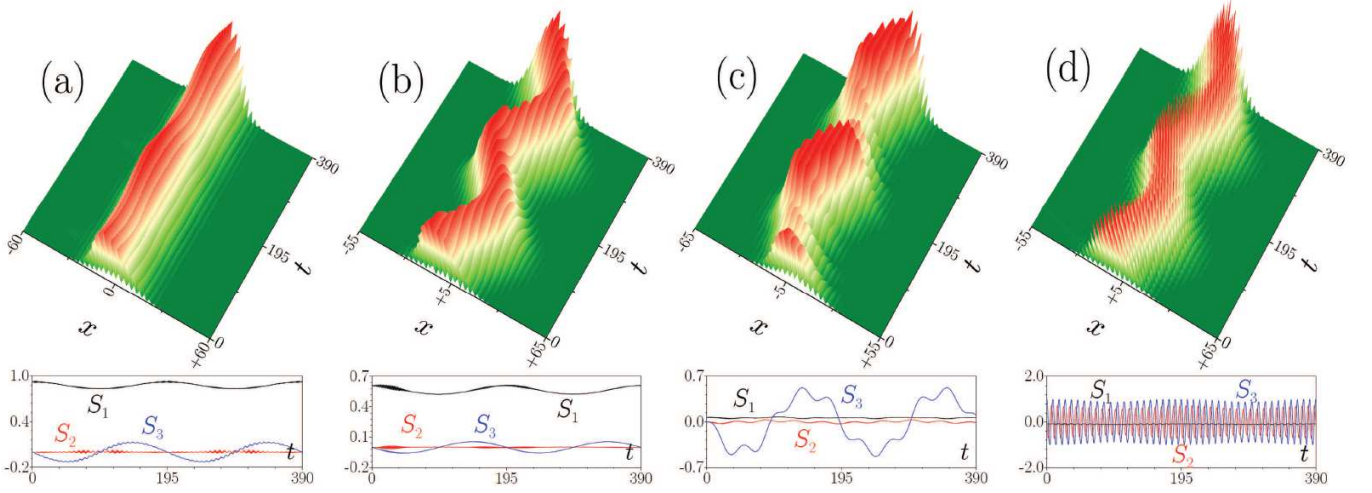


FIG. 3: (Color online) Dynamics of $|\Psi_1|$ in an OL for a broad wavepacket, with the width $w_{in} = 9\pi/2$, from the second-band for (a) $\gamma = 0.82$, (b) $\gamma = 1.85$, (c) $\gamma = 4.41$. (d) Amplitude of the in-phase superposition of the first- and second-band wavepackets for $\gamma = 1.85$ at $\beta = 2\Omega_1/31\pi$. The second row shows the evolutions of the spin components.

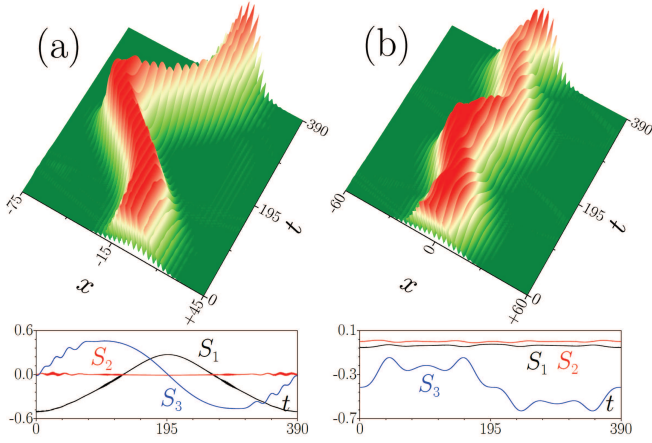


FIG. 4: (Color online) Dynamics of the amplitude $|\Psi_1|$ (upper panels) and evolution of the spin components (lower panels) for broad excitations, with $w_{in} = 9\pi/2$, from the first band at (a) $\gamma = 1.5$ (b) $\gamma = 5.0$ and $\beta = 2\Omega_1/31\pi$ in a ZL.

SO coupling, because one of the spinor components can be strongly suppressed at $\gamma \gg 1$ and the dynamics resembles that of the one-component system, as explained in [28].

An alternative approach to analyze the BOs is based on the calculation of the *localized* Wannier-Stark modes of the total Hamiltonian $H_0 + H_L + \beta x$ on numerically large windows with zero boundary conditions. For OLs such a spectrum (μ_n vs eigenvalue number n) is shown in Fig. 5(a). It reveals a specific WSL with *two* characteristic steps $\mu_{n+1} - \mu_n$ between neighboring eigenvalues. Due to the spinor character of the system the total WSL is a combination of two equidistant sub-ladders, namely μ_{n_1} and μ_{n_2} , shifted along μ . At $\gamma = 0$ the mutual

shift of the sub-ladders amounts to $2\Omega_1$. The Wannier-Stark modes from each sub-ladder have identical first and second components, and they are in-phase for one sub-ladder and out-of-phase in the other sub-ladder. If BOs and Rabi periods are commensurable, i.e., $2\Omega_1 = m\beta\pi$ at $\gamma = 0$, the two sub-ladders overlap exactly, the separation of the neighboring eigenvalues becomes equal to $\beta\pi$, and *any* excitation is recovered after the period $2/\beta$. At $2\Omega_1 = (m + 1/2)\beta\pi$ the *entire* ladder becomes equidistant with $\mu_{n+1} - \mu_n = \beta\pi/2$, and the period of BOs for any wavepacket exciting modes from *both* sub-ladders increases to $4/\beta$. At $\gamma \neq 0$ the SO coupling results in an additional mutual shift $\delta\mu$ of the two sub-ladders shown in Fig. 5(b). Due to such a shift the dynamics is in general non-periodic for inputs that excite *both* sub-ladders unless the SO coupling is selected such that $\delta\mu = m\pi\beta/2$ ($m \in \mathbb{N}$) and the equidistance of the entire spectrum is restored. If only *one* sub-ladder is excited the dynamics may still be periodic. In contrast to the behavior observed in OLs, the WSL for ZLs is equidistant for any γ with $\mu_{n+1} - \mu_n = \beta\pi/2$, which indicates BOs with a period $4/\beta$.

Summarizing, we have shown that SO coupling brings important new features into Bloch oscillations. It allows controlling the direction of atomic motion and enables nearly complete suppression of oscillations in OLs. In ZLs, oscillations feature period-doubling due to crossing of energy bands at the boundary of the Brillouin zone.

The work was supported by the FCT (Portugal) grant UID/FIS/00618/2013, by the Severo Ochoa Excellence program (Spain), and by Fundacio Cellex Barcelona.

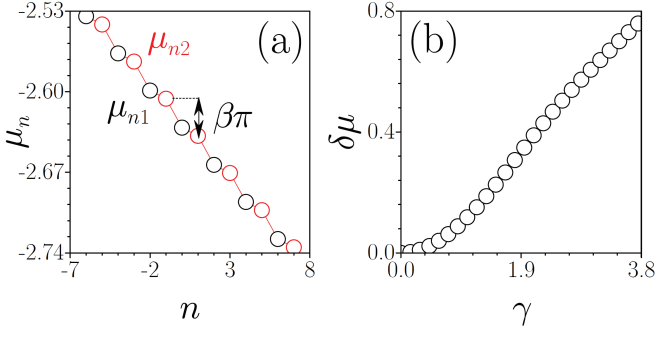


FIG. 5: (Color online) (a) Part of the WSL of an OL with $\gamma = 2$ and $\beta = 2\Omega_1/31\pi$. (b) Mutual shift of two sub-ladders in the spectrum, as a function of γ .

Supplemental Material for “Bloch oscillations in optical and Zeeman lattices in the presence of spin-orbit coupling”

Following the ideas of [1, 23], in this Supplemental Material we outline the derivation of the relation

$$\frac{dx_c}{dt} = \left. \frac{\partial \mu_{\alpha_0}(k)}{\partial k} \right|_{k=k_0-\beta t}, \quad (2)$$

which leads to Eq. (1) from the main text. In fact, we will address a slightly more general case: we consider the situation when the linear force β depends on time: $\beta = \beta(t)$. The particular case $\beta(t) = \text{const}$ obviously corresponds to the situation addressed in the main text. The derivation is valid for state described by a ket-vector $|\Psi\rangle$ of any dimension (i.e. having one, two or more components) and for the arbitrary strength of the SO-coupling γ (provided the Conditions formulated below are not violated).

We use the complete set of Bloch states $|k, \alpha\rangle$ of the Hamiltonian H : $H|k, \alpha\rangle = \mu_\alpha(k)|k, \alpha\rangle$, where $\mu_\alpha(k)$ is the energy of the state, the Bloch quasi-momentum k belongs to the reduced Brillouin zone (BZ): $k \in (-1, 1]$, and $\alpha = 1, 2, \dots$ is the band number ($\alpha = 1$ being the number of the lowest band). Following Houston’s approach [23], we introduce adiabatically-varying Bloch states $|\kappa(t), \alpha\rangle$ where

$$\kappa(t) = k - B(t), \quad B(t) = \int_0^t \beta(t') dt', \quad (3)$$

and k is the initial value of the quasi-momentum (or central quasi-momentum in the case of localized Bloch wavepackets). The spinor $|\Psi\rangle$ can be expanded in terms of the adiabatically-varying states as:

$$|\Psi\rangle = \sum_{\alpha=1}^{\infty} \int_{-1}^1 dk \chi_\alpha(k, t) |\kappa(t), \alpha\rangle. \quad (4)$$

and, for the sake of convenience, the spectral coefficients will be represented as

$$\chi_\alpha(k, t) = \chi_\alpha^{(0)}(k, t) e^{-i \int_0^t \mu_\alpha[\kappa(\tau)] d\tau} \quad (5)$$

with the functions $\chi_\alpha^{(0)}(k, t)$ to be determined latter. The normalization condition (in the direct and Fourier spaces)

$$\langle \Psi | \Psi \rangle = \sum_{\alpha=1}^{\infty} \int_{-1}^1 |\chi_\alpha(k, t)|^2 dk = 1 \quad (6)$$

is also imposed.

We assume that the following conditions hold:

Condition 1: Bloch states of only one band, say of the band α_0 , are initially excited, i.e. $\chi_\alpha(k, 0) = 0$ for $\alpha \neq \alpha_0$.

Condition 2: A wavepacket $|\Psi\rangle$ is a Bloch wave with a smooth and broad envelope (compared to the lattice period) and its spectrum centered at a quasi-momentum k_0 in the reduced BZ is much narrower than the BZ zone, so that the approximation

$$\int_{-1}^1 dk |\chi_{\alpha_0}(k, t)|^2 \frac{\partial \mu_{\alpha_0}(k)}{\partial k} \approx \frac{\partial \mu_{\alpha_0}(k_0)}{\partial k_0} \quad (7)$$

is valid [here we take into account the normalization (6)].

Condition 3: The linear force is weak, i.e., $|\beta(t)| \ll 1$, so that inter-band tunneling is negligible.

Let us start with the case $\beta \equiv 0$. Using the expansion

$$|\Psi\rangle = \sum_{\alpha=1}^{\infty} \int_{-1}^1 dk \chi_\alpha(k, t) |k, \alpha\rangle \quad (8)$$

where

$$\chi_\alpha(k, t) = \chi_\alpha^{(0)}(k) e^{-i \mu_\alpha(k) t}, \quad (9)$$

from the Schrödinger equation $i\Psi_t = (H_0 + H_L)\Psi$ one gets

$$\begin{aligned} i \frac{dx_c}{dt} &= \langle \Psi | [x, H_0 + H_L] | \Psi \rangle \\ &= \sum_{\alpha, \alpha'=1}^{\infty} \int_{-1}^1 dk' \int_{-1}^1 dk \chi_{\alpha'}^*(k', t) \chi_\alpha(k, t) \\ &\quad \times (\mu_\alpha(k) - \mu_{\alpha'}(k')) \langle k', \alpha' | x | k, \alpha \rangle. \end{aligned} \quad (10)$$

Using Floquet theorem, the Bloch states can be expressed in the form of the expansion

$$|k, \alpha\rangle = e^{ikx} \sum_{n=-\infty}^{\infty} \mathbf{c}_{\alpha, n}(k) e^{2inx} \quad (11)$$

where $\mathbf{c}_{\alpha, n}(k)$ are vector Fourier coefficients. The Bloch states are orthonormal, which implies

$$\sum_{m=-\infty}^{\infty} \mathbf{c}_{\alpha', m}^\dagger(k) \mathbf{c}_{\alpha, m}(k) = \delta_{\alpha\alpha'}. \quad (12)$$

Now, using (11) we get

$$\begin{aligned} \langle k', \alpha' | x | k, \alpha \rangle &= -2\pi i \sum_{m, n=-\infty}^{\infty} \mathbf{c}_{\alpha', m}^\dagger(k') \mathbf{c}_{\alpha, n}(k) \\ &\quad \times \frac{\partial}{\partial k} \delta(k - k' + 2n - 2m), \end{aligned} \quad (13)$$

and using the relation $-i\langle k', \alpha' | \frac{\partial}{\partial k} | k, \alpha \rangle$ we obtain

$$\begin{aligned} \langle k', \alpha' | \frac{\partial}{\partial k} H | k, \alpha \rangle &= \langle k', \alpha' | \frac{\partial}{\partial k} \mu_\alpha(k) | k, \alpha \rangle \\ &= \frac{\partial \mu_\alpha(k)}{\partial k} \delta_{\alpha\alpha'} \delta(k - k') + \mu_\alpha(k) \langle k', \alpha' | \frac{\partial}{\partial k} | k, \alpha \rangle. \end{aligned} \quad (14)$$

On the other hand, the same expression is computed as

$$\langle k', \alpha' | \frac{\partial}{\partial k} H | k, \alpha \rangle = \mu_{\alpha'}(k') \langle k', \alpha' | \frac{\partial}{\partial k} | k, \alpha \rangle \quad (15)$$

From (14) and (15) we obtain the useful relation

$$\begin{aligned} (\mu_{\alpha'}(k') - \mu_\alpha(k)) \langle k', \alpha' | \frac{\partial}{\partial k} | k, \alpha \rangle \\ = \frac{\partial \mu_\alpha(k)}{\partial k} \delta_{\alpha\alpha'} \delta(k - k'). \end{aligned} \quad (16)$$

Combining (16) and (10) we obtain

$$\frac{dx_c}{dt} = \sum_{\alpha=1}^{\infty} \int_{-1}^1 dk |\chi_\alpha(k, t)|^2 \frac{\partial \mu_\alpha(k)}{\partial k}. \quad (17)$$

Equation (17) is exact, no approximations were made so far. Using now the Conditions 1 and 2 formulated above, one arrives at the formula

$$\frac{dx_c}{dt} = \frac{\partial \mu_{\alpha_0}(k_0)}{\partial k_0}. \quad (18)$$

Let us now turn to the case when the field gradient is present, $\beta(t) \neq 0$. Following Houston's approach [23], we introduce adiabatically varying Bloch states $|\kappa(t), \alpha\rangle$, i.e. consider (11) with substitution $k \rightarrow \kappa(t)$, where

$$\kappa(t) = k - B(t), \quad B(t) = \int_0^t \beta(t') dt', \quad (19)$$

By direct differentiating and using that at each instant t , $|\kappa(t), \alpha\rangle$ are the eigenfunctions of H with $\mu_\alpha(\kappa(t))$ we obtain

$$i \frac{\partial |\Psi\rangle}{\partial t} = H |\Psi\rangle + \beta(t) x |\Psi\rangle + i |F\rangle \quad (20)$$

where

$$\begin{aligned} |F\rangle &= \sum_{\alpha=1}^{\infty} \int_{-1}^1 dk \left[\frac{\partial \chi_\alpha^{(0)}(k, t)}{\partial t} \psi_{\alpha, k} - \beta(t) \chi_\alpha^{(0)}(k, t) \frac{\partial \psi_{\alpha, k}}{\partial \kappa} \right] \\ &\quad \times \exp \left[-i \int_0^t \mu_\alpha(\kappa(\tau)) d\tau \right] e^{i\kappa(t)x} dk \end{aligned}$$

Now we require $\chi_\alpha^{(0)}(k, t)$, which, so far, are arbitrary functions of time, to ensure $|F\rangle = 0$. To this end we require $\langle \kappa, \alpha | F \rangle = 0$ for all α , which yields the set of equations

$$\begin{aligned} \frac{\partial \chi_\alpha^{(0)}(k, t)}{\partial t} &= \beta \sum_{\alpha'=1}^{\infty} \int_{-1}^1 dk' \chi_{\alpha'}^{(0)}(k', t) e^{i\Delta_{\alpha'\alpha}(\kappa', \kappa)} \\ &\quad \times \int_{-\infty}^{\infty} dx e^{i(k'-k)x} \psi_{\alpha, \kappa}^\dagger(x) \frac{\partial}{\partial \kappa'} \psi_{\alpha', \kappa'}(x), \end{aligned}$$

where $\kappa' = k' - B(t)$ and

$$\Delta_{\alpha'\alpha}(\kappa', \kappa) = \int_0^t [\mu_{\alpha'}(\kappa'(\tau)) - \mu_\alpha(\kappa(\tau))] d\tau \quad (21)$$

As we already did above, now we use the Fourier expansion (11) with the substitution $k \rightarrow \kappa(t)$ and obtain

$$\begin{aligned} \frac{\partial \chi_\alpha^{(0)}(k, t)}{\partial t} &= \beta(t) \sum_{\alpha'=1}^{\infty} \chi_\alpha^{(0)}(k, t) e^{i\Delta_{\alpha'\alpha}(\kappa, \kappa)} \\ &\quad \times \sum_{n=1}^{\infty} \mathbf{c}_{\alpha', n}^\dagger(\kappa) \frac{\partial}{\partial \kappa} \mathbf{c}_{\alpha, n}(\kappa). \end{aligned} \quad (22)$$

This is an exact formal result representing an infinite number of equations. If however all three conditions introduced above hold, Eq. (22) for a given band α can be approximated by

$$\frac{\partial \chi_\alpha^{(0)}(k, t)}{\partial t} \approx \beta(t) \sum_{\alpha'=1}^{\infty} \chi_{\alpha'}^{(0)}(k, t) \frac{\partial}{\partial \kappa} \sum_{n=1}^{\infty} \mathbf{c}_{\alpha', n}^\dagger(\kappa) \mathbf{c}_{\alpha, n}(\kappa). \quad (23)$$

Since at $\beta = 0$ we have the conservation (12), we conclude that

$$\frac{\partial}{\partial \kappa} \sum_{n=1}^{\infty} \mathbf{c}_{\alpha, n}^\dagger(\kappa) \mathbf{c}_{\alpha, n}(\kappa) = \mathcal{O}(\beta) \quad (24)$$

and thus one can use (18) with substitution $k_0 \rightarrow k_0 - B(t)$, leading to Eq. (2) at $\beta = \text{const}$.

-
- [1] F. Bloch, "Über die Quantenmechanik der Elektronen in Kristallgittern," Z. Phys. **52**, 555 (1928); C. Zener, "A theory of the electrical breakdown of solid dielectrics," Proc. R. Soc. A **145**, 523 (1934).
 - [2] J. Feldmann, K. Leo, J. Shah, D. B. A. Miller, J. E. Cunningham, S. Schmitt-Rink, T. Meier, G. von Plessen, A. Schulze, and P. Thomas, "Optical investigation of Bloch oscillations in a semiconductor superlattice," Phys. Rev. B **46** 7252 (1992); K. Leo, H. Bolivar, F. Brüggemann, R. Schwedler, and K. Köhler, "Observation of Bloch oscillations in a semiconductor superlattice," Solid State Commun. **84**, 943 (1992); C. Waschke, H. G. Roskos, R. Schwedler, K. Leo, H. Kurz, and Köhler, "Coherent submillimeter-wave emission from Bloch oscillations in a semiconductor superlattice," Phys. Rev. Lett. **70**, 3319 (1993).
 - [3] K. Leo, "Interband optical investigation of Bloch oscillations in semiconductor superlattices," Semicond. Sci. Technol. **13**, 249 (1998).
 - [4] E. E. Mendez, F. Agullo-Rueda, and J. M. Hong, "Stark localization in GaAs-GaAlAs superlattices under an electric field," Phys. Rev. Lett. **60**, 2426 (1988); P. Voisin, J. Bleuse, C. Bouche, S. Gaillard, C. Alibert, and A. Regreny, "Observation of the Wannier-Stark quantization in a semiconductor superlattice," Phys. Rev. Lett. **61**, 1639 (1988).

- [5] G. Nenciu, “Dynamics of band electrons in electric and magnetic fields: rigorous justification of the effective Hamiltonians,” *Rev. Mod. Phys.* **63**, 91 (1991); M. Glück, A. R. Kolovsky, and H. J. Korsch, “Wannier-Stark resonances in optical and semiconductor superlattices,” *Phys. Rep.* **366**, 103 (2002); A. Kolovsky and H. Korsch, “Bloch oscillations of cold atoms in optical lattices,” *Int. J. Mod. Phys. B* **18**, 1235 (2004).
- [6] E. Peik, M. B. Dahan, I. Bouchoule, Y. Castin, and C. Salomon, “Bloch oscillations of atoms, adiabatic rapid passage, and monokinetic atomic beams,” *Phys. Rev. A* **55**, 2989 (1997); E. Peik, M. Ben Dahan, I. Bouchoule, Y. Castin, C. Salomon, “Bloch oscillations and an accelerator for cold atoms,” *Appl. Phys. B* **65**, 685 (1997).
- [7] O. Morsch, J. H. Müller, M. Cristiani, D. Ciampini, and E. Arimondo, “Bloch oscillations and mean-field effects of Bose-Einstein condensates in 1D optical lattices,” *Phys. Rev. Lett.* **87**, 140402 (2001); M. Cristiani O. Morsch, J. H. Müller, D. Ciampini, and E. Arimondo, “Experimental properties of Bose-Einstein condensates in one-dimensional optical lattices: Bloch oscillations, Landau-Zener tunneling, and mean-field effects,” *Phys. Rev. A* **65**, 063612 (2002).
- [8] U. Peschel, T. Pertsch, and F. Lederer, “Optical Bloch oscillations in waveguide arrays,” *Opt. Lett.* **23**, 1701 (1998); T. Pertsch, P. Dannberg, W. Elfle, A. Bräuer, and F. Lederer, “Optical Bloch oscillations in temperature tuned waveguide arrays,” *Phys. Rev. Lett.* **83**, 4752 (1999); R. Morandotti, U. Peschel, J. S. Aitchison, H. S. Eisenberg, and Y. Silberberg, “Experimental observation of linear and nonlinear optical Bloch oscillations,” *Phys. Rev. Lett.* **83**, 4756 (1999).
- [9] H. Trompeter, W. Krolikowski, D. N. Neshev, A. S. Desyatnikov, A. A. Sukhorukov, Y. S. Kivshar, T. Pertsch, U. Peschel, and F. Lederer, “Bloch oscillations and Zener tunneling in two-dimensional photonic lattices,” *Phys. Rev. Lett.* **96**, 053903 (2006).
- [10] R. Sapienza, P. Costantino, D. Wiersma, M. Ghulinyan, C. J. Oton, and L. Pavesi, “Optical analogue of electronic Bloch oscillations,” *Phys. Rev. Lett.* **91**, 26 (2003).
- [11] A. Block, C. Etrich, T. Limboeck, F. Bleckmann, E. Söergel, C. Rockstuhl, and S. Linden, “Bloch oscillations in plasmonic waveguide arrays,” *Nat. Commun.* **5**, 3843 (2014).
- [12] J. Dalibard, F. Gerbier, G. Juzeliunas, and P. Öhberg, “Artificial gauge potentials for neutral atoms,” *Rev. Mod. Phys.* **83**, 1523 (2011).
- [13] Y.-J. Lin, R. L. Compton, K. Jiménez-García, W. D. Phillips, J. V. Porto and I. B. Spielman, “A synthetic electric force acting on neutral atoms,” *Nature Phys.* **7**, 531 (2011).
- [14] Y.-J. Lin, R. L. Compton, K. Jiménez-García, J. V. Porto, and I. B. Spielman, “Synthetic magnetic fields for ultracold neutral atoms,” *Nature* **462**, 628, (2009).
- [15] M. Atala, M. Aidelsburger, J. T. Barreiro, D. Abanin, T. Kitagawa, E. Demler, and I. Bloch, “Direct measurement of the Zak phase in topological Bloch bands,” *Nat. Phys.* **9**, 795 (2013); C. J. Kennedy, G. A. Siviloglou, H. Miyake, W. C. Burton, and W. Ketterle, “Spin-orbit coupling and quantum spin Hall effect for neutral atoms without spin flips,” *Phys. Rev. Lett.* **111**, 225301 (2013).
- [16] J. Struck, C. Ölschläger, M. Weinberg, P. Hauke, J. Simonet, A. Eckardt, M. Lewenstein, K. Sengstock, and P. Windpassinger, “Tunable gauge potential for neutral and spinless particles in driven optical lattices,” *Phys. Rev. Lett.* **108**, 225304 (2012).
- [17] D. Witthaut, “Quantum walks and quantum simulations with Bloch-oscillating spinor atoms,” *Phys. Rev. A* **82**, 033602 (2010).
- [18] Y. Ke, X. Qin, H. Zhong, J. Huang, C. He, and C. Lee, “Bloch-Landau-Zener dynamics in single-particle Wannier-Zeeman systems,” *Phys. Rev. A* **91**, 053409 (2015).
- [19] Y. J. Lin, K. Jiménez-García, and I. B. Spielman, “Spin-orbit-coupled Bose-Einstein condensates,” *Nature* **471**, 83 (2011); V. Galitski and I. B. Spielman, “Spin-orbit coupling in quantum gases,” *Nature* **494**, 49 (2013); X. Zhou, Y. Li, Z. Cai, and C. Wu, “Unconventional states of bosons with synthetic spin-orbit coupling,” *J. Phys. B* **46**, 134001 (2013).
- [20] J. Larson, J.-P. Martikainen, A. Collin, and E. Sjöqvist, “Spin-orbit-coupled Bose-Einstein condensate in a tilted optical lattice,” *Phys. Rev. A* **82**, 043620 (2010).
- [21] R. A. Caetano, “Nontrivial Bloch oscillation and Zener tunneling frequencies in helicoidal molecules due to spin-orbit coupling,” *Phys. Rev. B* **89**, 195414 (2014).
- [22] K. Jiménez-García, L. J. LeBlanc, R. A. Williams, M. C. Beeler, A. R. Perry, and I. B. Spielman, “Peierls substitution in an engineered lattice potential,” *Phys. Rev. Lett.* **108**, 225303 (2012).
- [23] W. V. Houston, “Acceleration of electrons in a crystal lattice,” *Phys. Rev.* **57**, 184 (1940).
- [24] The derivation of the evolution equations for the expectation value of the position of an atom for a multicomponent case is outlined in the Supplemental material.
- [25] After submission of our manuscript the paper H. Chen, X.-J. Liu, and X. C. Xie, “Hidden nonsymmorphic symmetry in optical lattices with one-dimensional spin-orbit coupling,” *Phys. Rev. A* **93**, 053610 (2016) was published, where an analysis of the band-gap spectra of spin-1/2 fermions in an OL in the presence of SO coupling and a tunable ZL is presented, revealing symmetries of the system involving point groups and translations.
- [26] V. E. Lobanov, Y. V. Kartashov, and V. V. Konotop, “Fundamental, multipole, and half-vortex gap solitons in spin-orbit coupled Bose-Einstein condensates,” *Phys. Rev. Lett.* **112**, 180403 (2014).
- [27] Y. Zhang and C. Zhang, “Bose-Einstein condensates in spin-orbit-coupled optical lattices: Flat bands and superfluidity,” *Phys. Rev. A* **87**, 023611 (2013).
- [28] C. Li, F. Ye, Y. V. Kartashov, V. V. Konotop, and X. Chen, “Localization-delocalization transition in spin-orbit-coupled Bose-Einstein condensate,” *Sci. Rep.* **6**, 31700 (2016).